The Fingerprint of Climate Trends on European Crop Yields: Supplementary Information Appendix

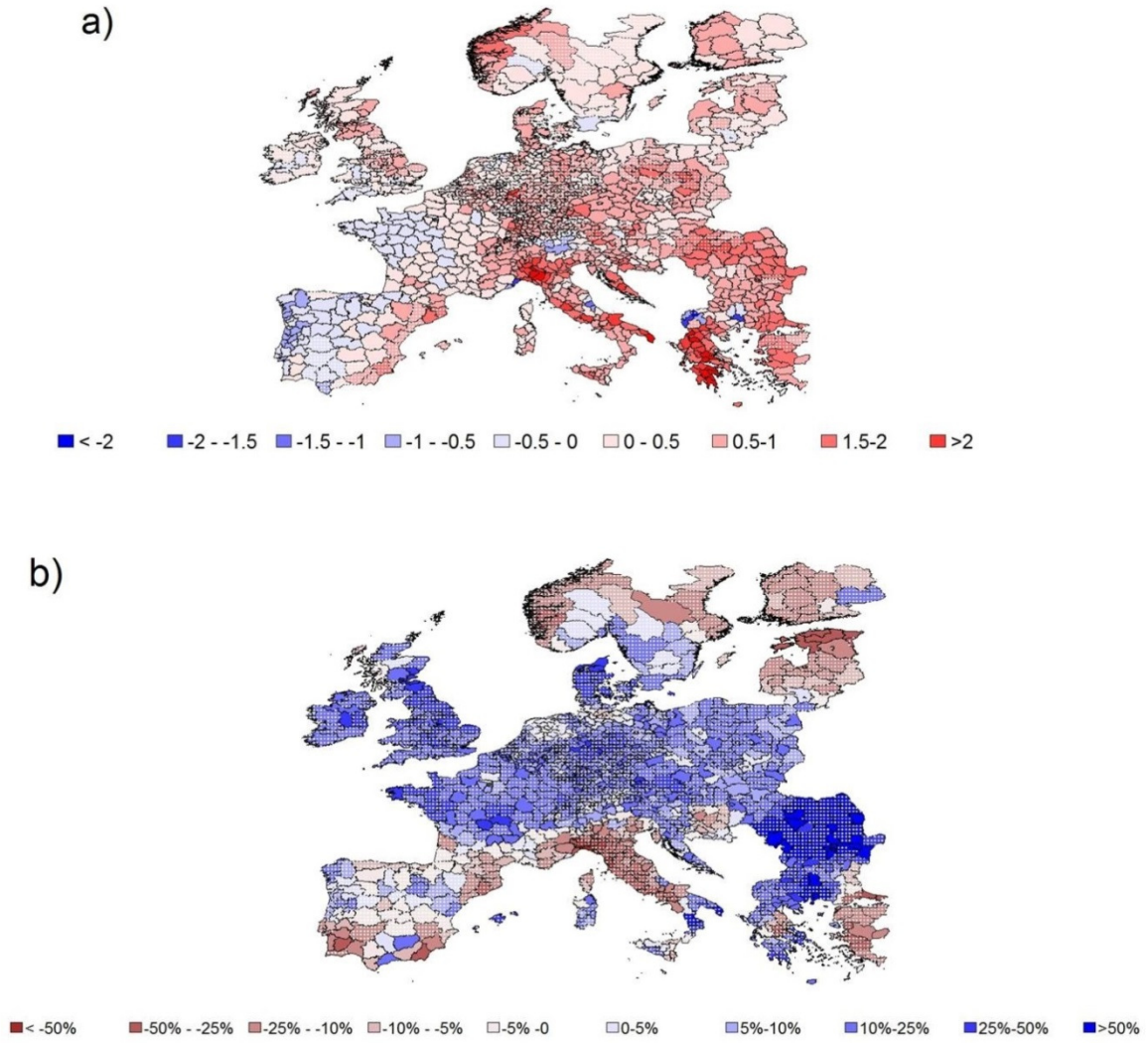

Figure S1: March – September temperature (°C) and precipitation (mm per month) changes over Europe based on linear time trends 1989-2009(1, 2). White stippling shows regions where the long-term trend is not statistically significant at the 10% level.

Crop	Countries Included
Wheat	Belgium, France, Germany, Greece, Ireland, Italy, Luxembourg, Netherlands, Portugal, Spain, UK.
Maize	Belgium, France, Germany, Greece, Italy, Netherlands, Portugal, Spain.
Barley	Belgium, France, Germany, Greece, Ireland, Italy, Luxembourg, Netherlands, Portugal, Spain, UK.
Sugarbeet	Belgium, France, Germany, Greece, Italy, Netherlands, Spain, UK.

Table S1: Countries with regions included in this study. The spatial extent of the study is limited by the need for a sufficient length of data from which to calculate a reliable estimate of the long-term yield trend (set at 10 years) and the limited generalizability of the yield-response model. For these reasons, eastern Europe is not included in the analysis.

Supplementary Methods

1. Estimation of Long- and Short-Run Response Curves
2. Bootstrap of the Null Distribution
3. Power Simulation Analysis

1. Estimation of Long- and Short-Run Response Curves

The short- and long-run responses of yield to temperature and precipitation changes are jointly estimated using panel data. Our source of economic and yield data is the EU Farm Accountancy Data Network (FADN) survey between 1989 and 2009, aggregated from the farm to the regional (sub-national) level (3). Yields are calculated as the crop produced in the year divided by the area of crop planted. Weather and climate data are monthly means averaged over the growing season defined using the observed planting and harvest dates for each region (for winter crops, the 4 months prior to the observed harvest date) (1, 2, 4).

The yields across Europe are modelled as a quadratic in average growing-season temperature and average growing-season precipitation using the same response function across the region. All time-trending variables are first de-trended using linear time-trends for each sub-national region. This step removes all long-term trends (the source of variation used for Tests 1 and 2 presented in this paper) and thus avoids any risk that the same data is being used to both train the response model and test for evidence of climate trend impacts.

De-trended log yields (Y) for sub-national region i, in country j in year t are estimated as:

$$Y_{ijt} = \theta_0 + \boldsymbol{\theta_1}\overline{W}_{ij} + \boldsymbol{\theta_2}\overline{W}_{ij}^2 + \boldsymbol{\theta_3}(W_{ijt} - \overline{W}_{ij})^2 + \theta_{4,j}Country_j + \boldsymbol{\theta_5}Controls_{ijt} + \varepsilon_{ijt} \qquad (Eq\ S1)$$

where W_{ijt} is a vector that includes growing season temperature and precipitation and $\overline{W}_{ij}$ is the 30-year climatological average over the baseline period (1958-1988). Bold denotes vectors of coefficients. Our de-trending step removes the effect of unobserved time-trends at the sub-national region level. We control for unobserved time-constant variation between countries using a country fixed effect and other observed within-country variation using a suite of controls. These include a vector of soil-quality variables (organic carbon content, water-holding capacity, erodibility, and soil type), altitude and altitude squared, subsidies received per Ha, and irrigated area per Ha (5). This equation is estimated using OLS regression, weighting by the square root of crop area to reduce heteroskedasticity and to make results more representative of the average growing area. This method uses cross-sectional variation in baseline climate to estimate the long-run response of yields to changing climate and inter-temporal deviations in growing-season weather from baseline climate to estimate the short-run impact of weather shocks. It is very similar to the method described in Moore and Lobell (6), but with the added initial step of de-trending at the sub-national level. This results in nearly identical coefficients but explicitly removes any concerns of training and testing on the same data.

Given a change in climate in region i from $\overline{W}_{0i}$ to $\overline{W}_{1i}$, the long-run response $\left(\Delta\hat{Y}_{LR}\right)$is defined as:

$$\Delta\hat{Y}_{LRi} = \widehat{\boldsymbol{\theta_1}}(\overline{W}_{1i} - \overline{W}_{0i}) + \widehat{\boldsymbol{\theta_2}}\left(\overline{W}_{1i}^2 - \overline{W}_{0i}^2\right)$$

Because the parameters of this response function are estimated using cross-sectional variation in the 30-year mean baseline climate, this relationship between climate and yields implicitly includes all adaptations used by farmers within the region. This is under the assumption that farmers have fully adjusted to their baseline climate and that the relative prices of crops and inputs has remained constant (7). The short-run response ($\Delta\hat{Y}_{SR}$) is defined as:

$$\Delta\hat{Y}_{SRi} = \widehat{\boldsymbol{\theta_1}}(\overline{W}_{1i} - \overline{W}_{0i}) + \widehat{\boldsymbol{\theta_2}}\left(\overline{W}_{1i}^2 - \overline{W}_{0i}^2\right) + \widehat{\boldsymbol{\theta_3}}(\overline{W}_{1i} - \overline{W}_{0i})^2$$

This is the same as $\Delta\hat{Y}_{LR}$ but includes the additional term $\widehat{\boldsymbol{\theta_3}}(\overline{W}_{1i} - \overline{W}_{0i})^2$, which can be interpreted as a penalty associated with being imperfectly adjusted to the new climate, $\overline{W}_{1i}$, which is different from the expected baseline climate, $\overline{W}_{0i}$ (since the estimated $\widehat{\boldsymbol{\theta_3}}$ is negative). This penalty term is estimated using inter-annual weather fluctuations ($W_{ijt} - \overline{W}_{ijt}$) in the panel data-set (Eq S1). Since these weather fluctuations are transient and at least partly unanticipated, farmers have a more limited set of adjustments than are employed in response to long-term climatic differences. Figure S2 gives a diagrammatic representation of these short- and long-term response curves under the parametric assumptions of the estimating equation.

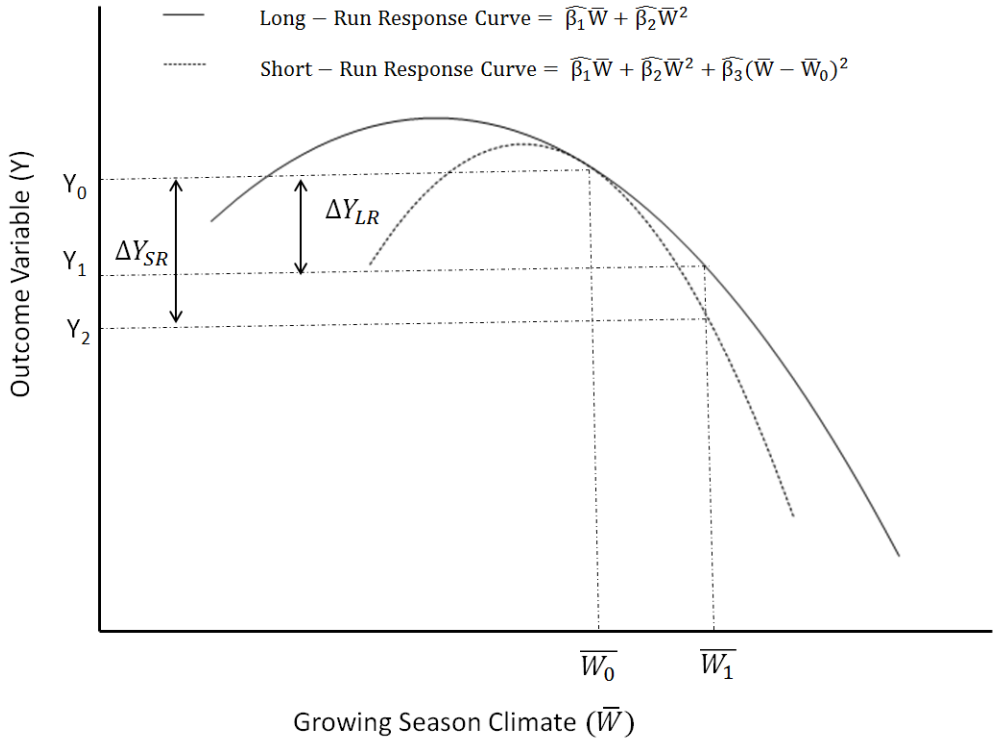

Figure S2: Diagrammatic representation of short- and long-run responses to a shift in climate from $\overline{W}_0$to $\overline{W}_1$ given the functional-form assumptions of the estimating equation (Equation S1).

Figures S3 and S4 show the temperature and precipitation response curves used in this paper. Standard errors for the parameters of these response curves are estimated using 500 block-bootstraps, blocking at the country by two-year level to account for heteroskedasticity, within-country spatial autocorrelation, and temporal autocorrelation at one-year lag and are given in Table S2. A fuller description of this estimation procedure, robustness checks, and standard errors can be found in Moore & Lobell (6).

	Wheat Yield	Maize Yield	Barley Yield	Sugarbeet Yield
	(1)	(1)	(1)	(1)
Mean Temp	0.1552 *	0.0137	0.1655 ***	0.3482 ***
	0.078	0.020	0.0433	0.068
Mean Temp^2	-0.017 ***	0.0000	-0.012 ***	-0.011 ***
	0.003	0.0006	0.002	0.002
(Temp-Mean Temp)^2	-0.0181 *	-0.0299 ***	-0.0287 ***	-0.0252 ***
	0.0073	0.0086	0.006	0.004
Mean Precip	0.0168 ***	0.0085 ***	0.001	0.0032 **
	0.0022	0.001	0.0021	0.001
Mean Precip^2	-5.09E-05 ***	-3.18E-05 ***	-8.73E-06	-6.16E-06
	8.78E-06	4.56E-06	7.80E-06	4.47E-06
(Precip-Mean Precip)^2	-2.35E-05	-2.02E-05 ·	-2.46E-05 ·	-8.60E-06
	1.69E-05	1.11E-05	1.30E-05	1.20E-05

· p<0.1; *p<0.05; **p<0.01;***p<0.001

Table S2: Response function coefficients for the response model shown in Equation S1 and standard errors based on 500 block-bootstraps with blocks defined at the country by two-year level to account for heteroskedasticity, spatial autocorrelation and temporal autocorrelation with one year lag.

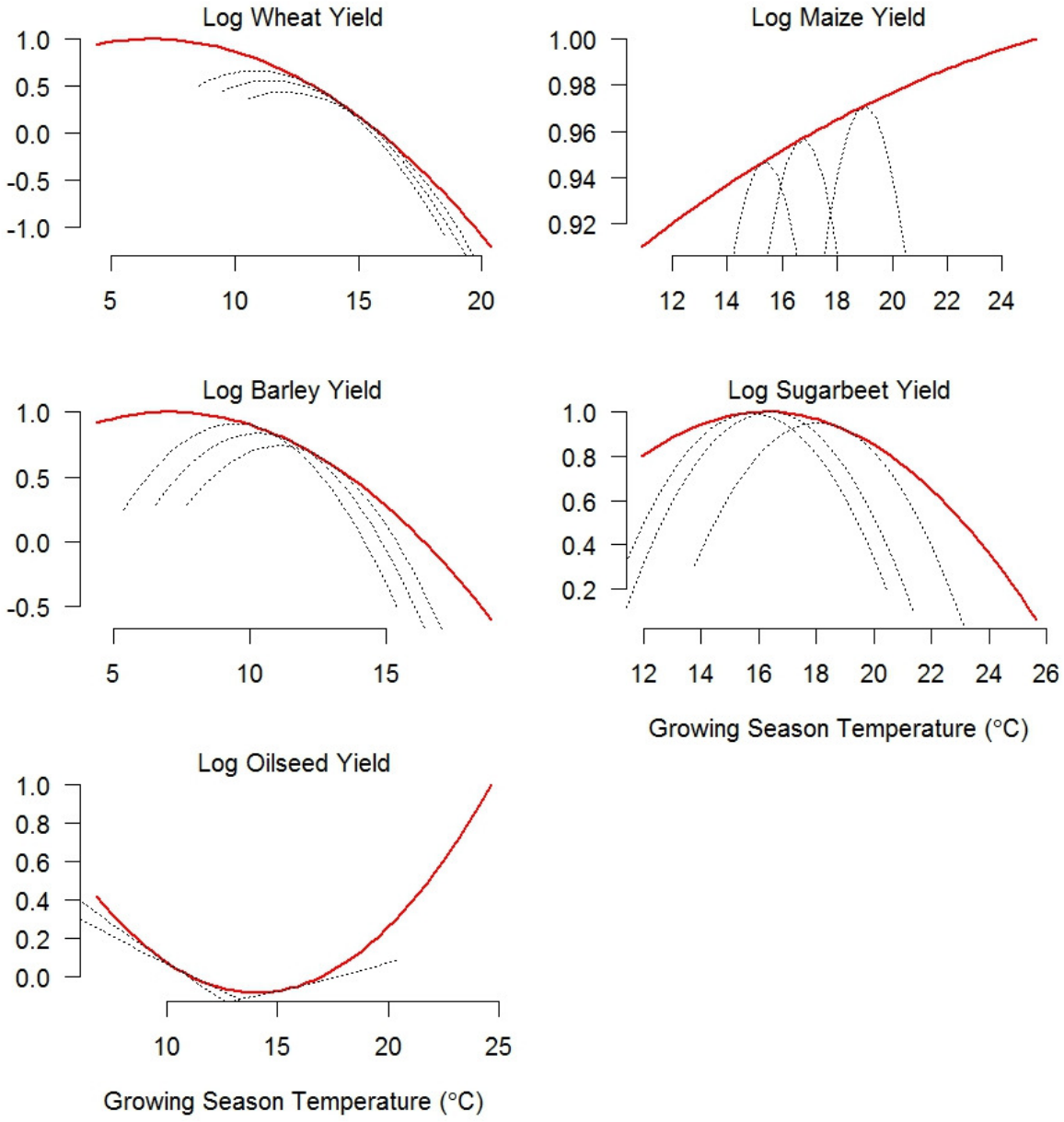

Figure S3: Graphical depiction of the long-run (red solid line) and short-run (black dotted line) relationship between de-trended yields and de-trended growing season temperature estimated using Equation S1. The range of the x-axis corresponds to the range of growing season temperature in each panel dataset. The three examples of short-run relationships are plotted centered at the 25th, 50th, and 75th percentiles of growing-season temperature. Curves are shifted along the y-axis so that the maximum value over the plotting range is 1. Because the dependent variable is logged, movement along the y-axis represents a % change in the outcome variable.

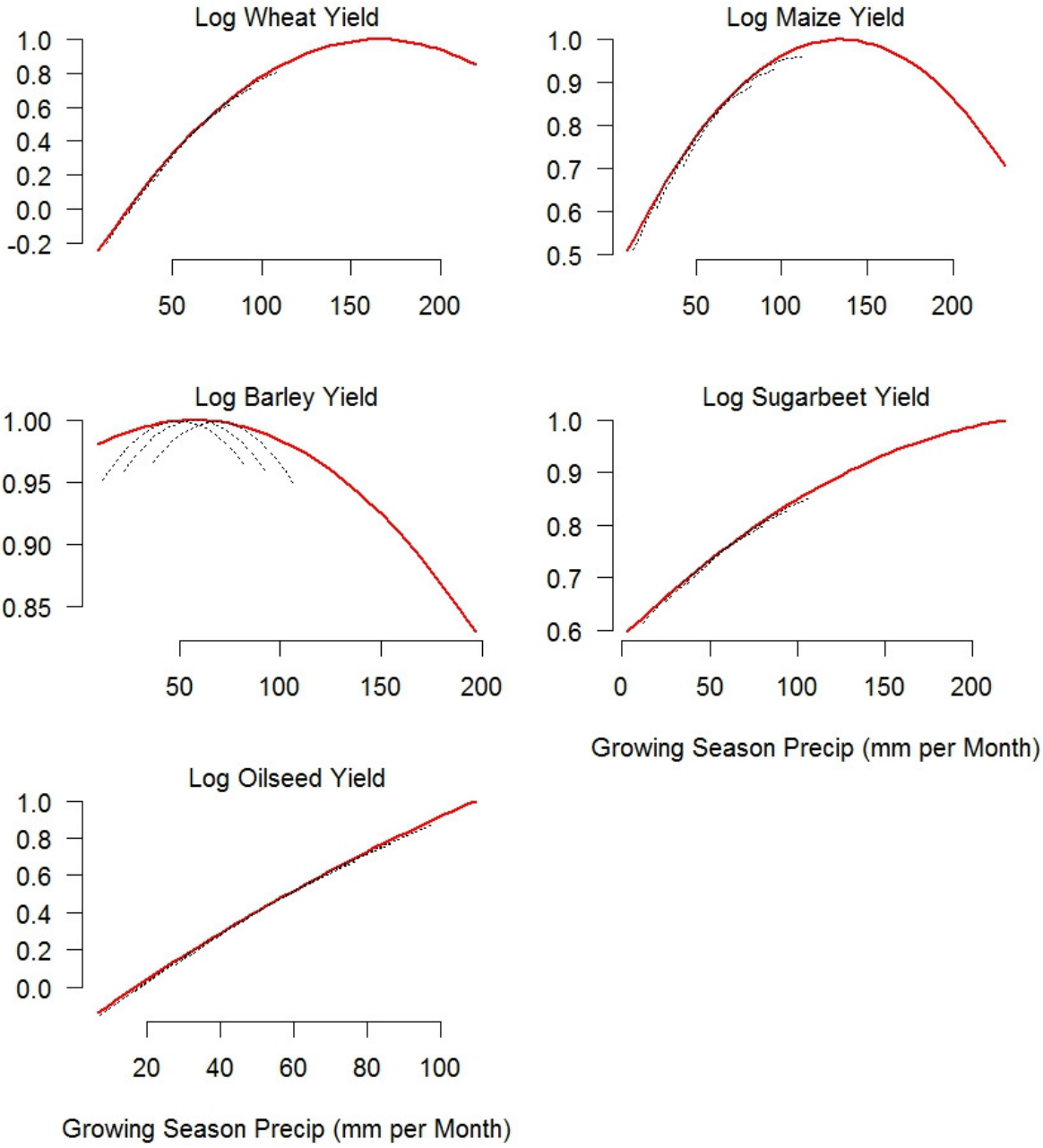

Figure S4: Graphical depiction of the long-run (red solid line) and short-run (black dotted line) relationship between de-trended yields and de-trended growing season precipitation estimated using Equation S1. The range of the x-axis corresponds to the range of growing season precipitation in each panel dataset. The three examples of short-run relationships are plotted centered at the 25th, 50th, and 75th percentiles of growing-season precipitation. In many cases the short-run response curves are not visible because they overlie the long-run response curves. Curves are shifted along the y-axis so that the maximum value over the plotting range is 1. Because the dependent variable is logged, movement along the y-axis represents a % change in the outcome variable.

2. Bootstrap of the Null Distribution

The procedures used to estimate the distribution of the test statistics under the null hypotheses are described in the Methods section, but a step-by-step procedure is provided here for additional clarity. For both tests, the procedure accounts for uncertainty in the estimation of the yield response function by resampling the parameters of the response function from their joint multivariate normal distribution estimated using the block-bootstrap described in the previous section.

Test 1

1. Estimate the regression shown in Equation 1 (Main Text) to give the coefficient estimate $\hat{\beta}_1$
2. Estimate $Var(\hat{\beta}_1)$:
    i. Resample the parameters of the response function ($\boldsymbol{\theta_{1\_b}}$ and $\boldsymbol{\theta_{2\_b}}$) from their joint distribution
    ii. Recalculate predicted yield trends using these parameters
    iii. Resample the data by country
    iv. Recalculate $\hat{\beta}$
    v. Repeat 2.i to 2.iv 500 times and take the variance of these estimates
3. Calculate the test statistic $\tau_1 = \frac{\widehat{\beta_1}}{\sqrt{\widehat{Var}(\widehat{\beta}_1)}}$
4. Resample the parameters of the response function
5. Recalculate predicted yield trends using these parameters
6. Resample the data by country
7. Calculate the bootstrapped estimate $\hat{\beta}_{1\_b}$
8. Estimate $Var(\hat{\beta}_{1\_b})$ by repeating steps 2.i – 2.v using the bootstrapped sample
9. Calculate the bootstrapped test statistic, imposing the null hypothesis $\tau_{1\_b} = \frac{\widehat{\beta}_{1\_b} - \widehat{\beta_1}}{\sqrt{\widehat{Var}(\widehat{\beta}_1)}}$
10. Repeat 4-9 500 times
11. Fine the 95th quantile of the distribution to give the critical value for the (one-sided) test of size 5%.

This is a version of bootstrap-t procedure using a double-bootstrap described by both MacKinnon (8) and Cameron, Gelbach and Miller (9). Block-bootstrapping by country accounts for both heteroskedasticity and correlation of the error terms within countries while directly bootstrapping the t-statistic provides improved inference in cases with relatively few clusters (countries), as is the case here (9). Resampling the parameters of the response function and recalculating the predicted trends accounts for the fact that the climate-yield response function is not known exactly.

Test 2

1. Estimate Equations 2 and 3 (Main Text) and calculate $\tau_2 = \frac{RSS_2 - RSS_3}{RSS_3/(n-3)}$

2. Resample the parameters of the response function ($\boldsymbol{\theta_{1\_b}}$ and $\boldsymbol{\theta_{2\_b}}$) from the joint distribution
3. Recalculate predicted yield trends using these parameters
4. Resample the data by country
5. Calculate the bootstrapped estimate τ_{2_b}, imposing the null hypothesis:
    i. Calculate RSS_{2_b} from the resampled data
    ii. Calculate the mean and variance of the difference between the long-run and short-run predicted trends in the resampled data
    iii. From the resampled data, regress the observed trends on the short-run predicted trends and a random variable with the same mean and variance calculated in 5.ii
    iv. Use the residuals from this regression to calculate RSS_{3_b}
    v. $\tau_{2\_b} = \frac{RSS_{2\_b} - RSS_{3\_b}}{RSS_{3\_b}/(n-3)}$
6. Repeat 2-5 500 times
7. Find the 95th quantile of the distribution to give the critical value for a (one-tailed) test of size 5%.

This procedure both accounts for uncertainty in the response function through the resampling of parameters, and potential heteroskedasticity and spatial autocorrelation. The bootstrapping procedure imposes the null hypothesis (that the additional variable in the second, unrestricted regression has no explanatory power) by adding a random variable rather than the true variable, therefore giving the sampling variability of τ_2 under the null hypothesis.

3. Power Simulation Analysis

The goal of the power simulation analysis was to determine under what conditions Test 1 and Test 2 might be expected to have sufficient power (>80%) for reliable inference. Because of computational limitations, a single long-run response function was used (the sugarbeet temperature response function, Table S2). This gives a moderately sensitive, non-linear response to warming over the region of interest (Fig S3) and therefore might be expected to give higher power compared to flatter or more linear response functions. For each parameter that might affect statistical power, a high and low value were determined based on realistic values informed by the European dataset. Additional levels of noise were included because of the importance of this parameter. These parameters were combined in a full factorial design for the power simulation.

Parameter	Fixed Value	V. Low Value	Low Value	Mid Value	High Value
Magnitude Climate Trend	--	--	0.5°C	--	5°C
Variance Climate Trend	--	--	$0.5°C^2$		$2°C^2$
Theta1	$0.348°C^{-1}$	--	--	--	--
Theta2	$-0.011°C^{-2}$	--	--	--	--
Theta3	--	--	$-0.005°C^{-1}$	--	$-0.03°C^{-1}$
Variance Baseline Climate	--	--	$2°C^2$	--	$6°C^2$
Noise Variance	--	0.05	0.5	1	5
Response Function Uncertainty	$\begin{bmatrix} 4.56*10^{-3} & -1.40*10^{-4} \\ -1.40*10^{-4} & 4.32*10^{-6} \end{bmatrix}$	--	--	--	--
Sample Size	125	--	--	--	--
Test Size	5%	--	--	--	--

Table S3: Parameter values used in the power simulation analysis. These were combined in a full factorial design and power was calculated using 200 simulations for each combination of parameters. The response function parameters (Theta1 and Theta2) and their variances were taken from the sugarbeet temperature response function (Figure S3).

Each simulation involved drawing a sample of 125 hypothetical baseline climates and climate trends from two independent normal distributions defined by the parameters in Table S3 (the mean of the baseline climates was fixed at 17°C, the optimum of the sugarbeet yield response curve). Yield trends were predicted with and without adaptation using the long- and short-run yield response functions respectively. Then "observed" yield trends were generated by adding white noise (with a variance defined in Table S3) to the predicted long-run trends, representing the variation in yield trends not explained by climate trends or other control variables. Tests 1 and 2 were then performed, with the distribution of the test statistics under the null estimated using the simulated data as described in Methods and the SI. This was repeated 200 times for each combination of parameter values to determine the probability of rejecting the null hypothesis, equivalent to the power of the test since the alternative hypothesis is true in the simulations by construction. Results are given in Figure S5 (Test 1) and Figure S6 (Test 2).

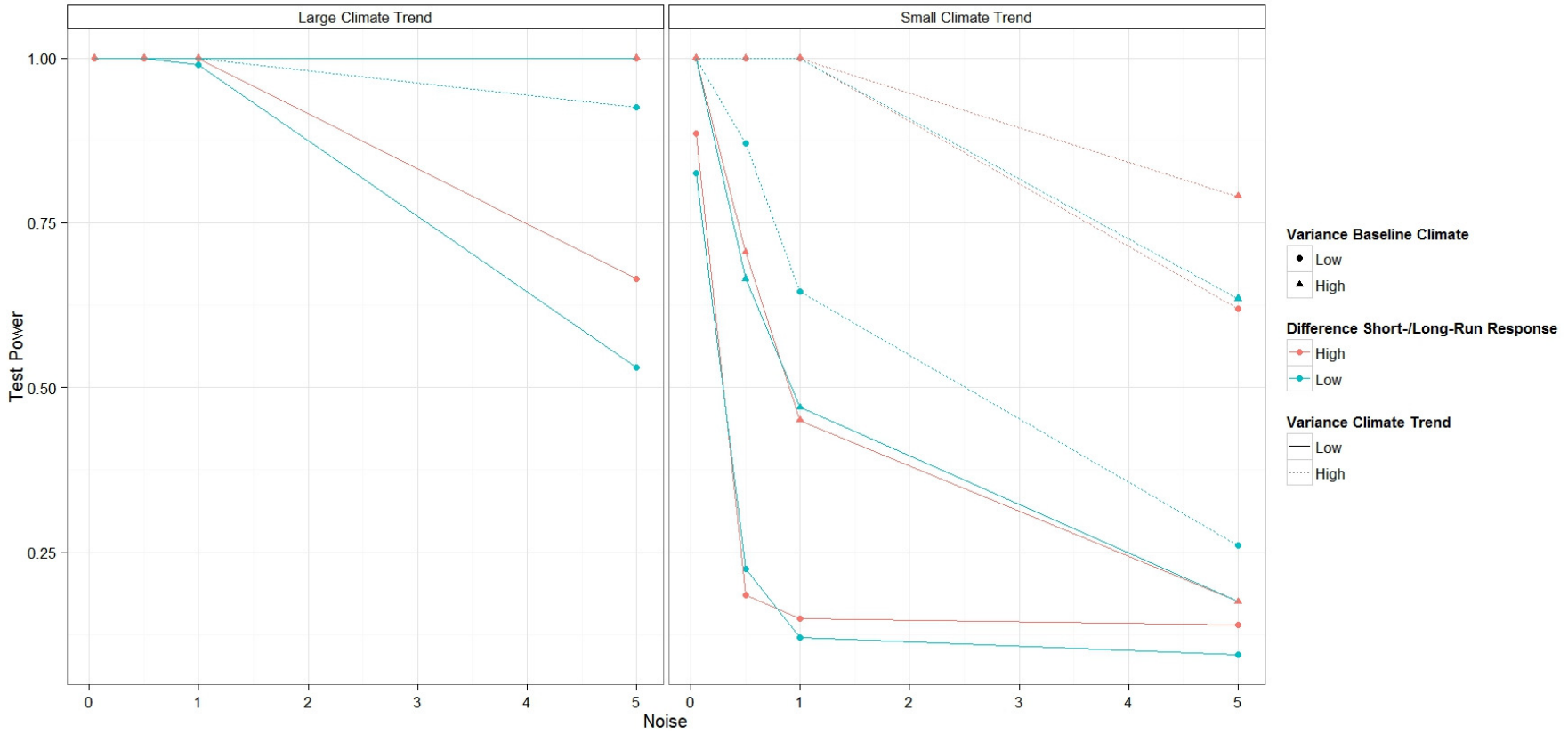

Figure S5: Simulated power (probability of rejecting the null hypothesis, conditional on the alternative being true) of Test 1 (detection of climate change impacts) under various parameter combinations. Power is consistently high when the climate trend is large (5°C) and can be high even if the climate trend is small (0.5°C) in certain contexts. Power is based on 200 simulations for each combination of parameter values and inference is made using 200 bootstraps for each simulation. Parameter values used for the simulation are shown in Table S3.

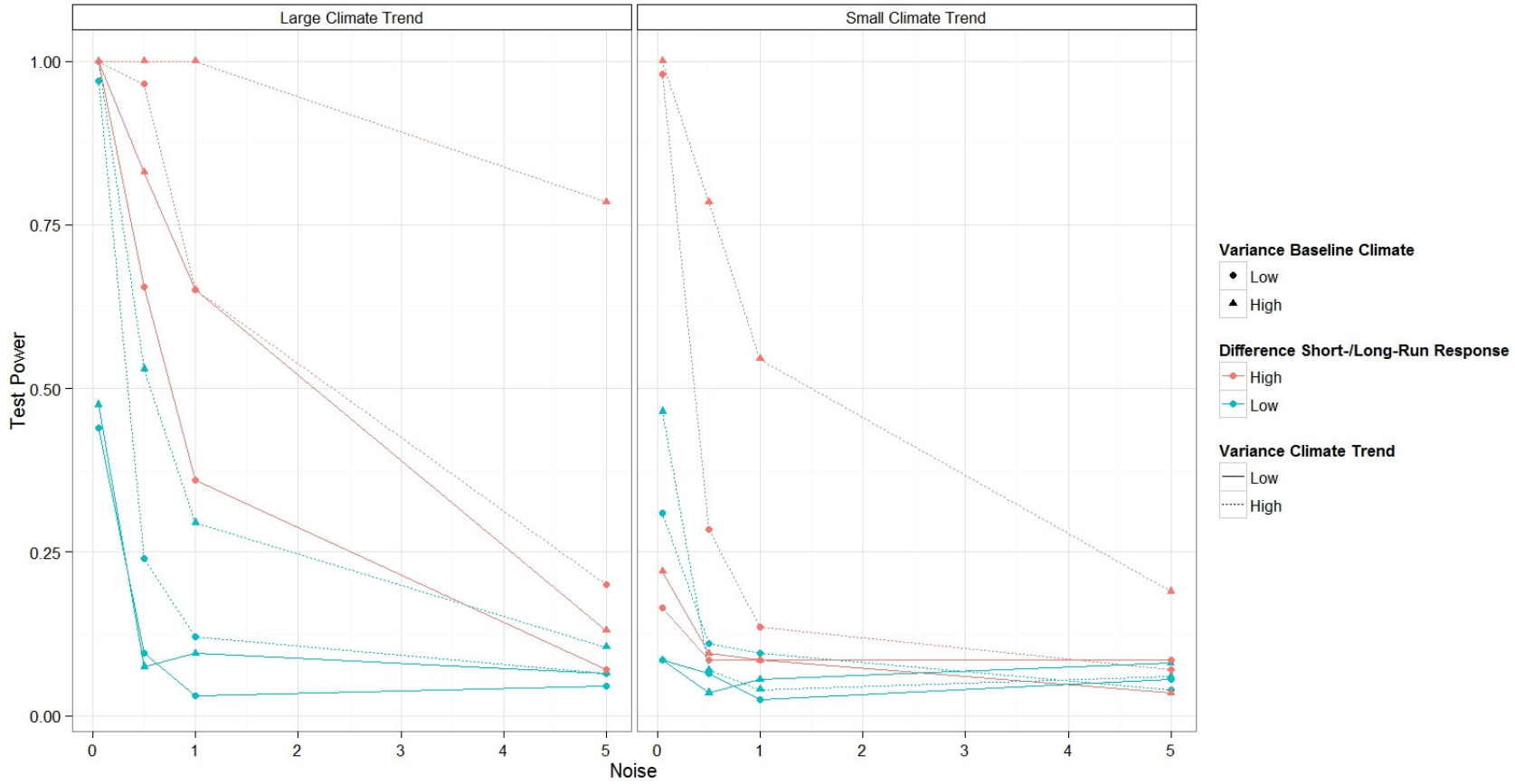

Figure S6: Simulated power (probability of rejecting the null hypothesis, conditional on the alternative being true) of Test 2 (detection of climate change adaptation) under various parameter combinations. Power is consistently low, even when the climate trend is large. Power is based on 200 simulations for each combination of parameter values and inference is made using 200 bootstraps for each simulation. Parameter values used for the simulation are shown in Table S3.

Parameter	Units	Log Wheat Yield	Log Maize Yield	Log Barley Yield	Log Sugarbeet Yield	Log Oilseed Yield
Mean Temperature Trend	°C per 20 years	0.97	0.77	0.75	0.68	0.60
Variance Temperature Trend	(°C per 20 years)^2	0.24	0.51	0.20	0.37	0.16
Mean Precipitation Trend	mm per Month per 20 years	4.4	-2.1	4.6	4.0	8.4
Variance Precipitation Trend	(mm per Month per 20 years)^2	198	289	143	320	104
Variance Baseline Temperature	°C^2	2.8	5.4	3.6	6.6	13.7
Variance Baseline Precipitation	(mm per Month)^2	554	904	458	737	161
Noise Variance	(% per 20 Years)^2	8.2	13.1	5.0	5.8	19.6

Table S4: Parameters used to estimate power of Tests 1 and 2 for 5 European crops. Temperature and precipitation values are calculated for the crop- and region-specific growing seasons defined using observed planting and harvest dates(4). Noise was calculated based on the variance of residuals from a regression of the observed trend on all explanatory variables (predicted climate trend, trend in coupled subsidies, and trend in prices).

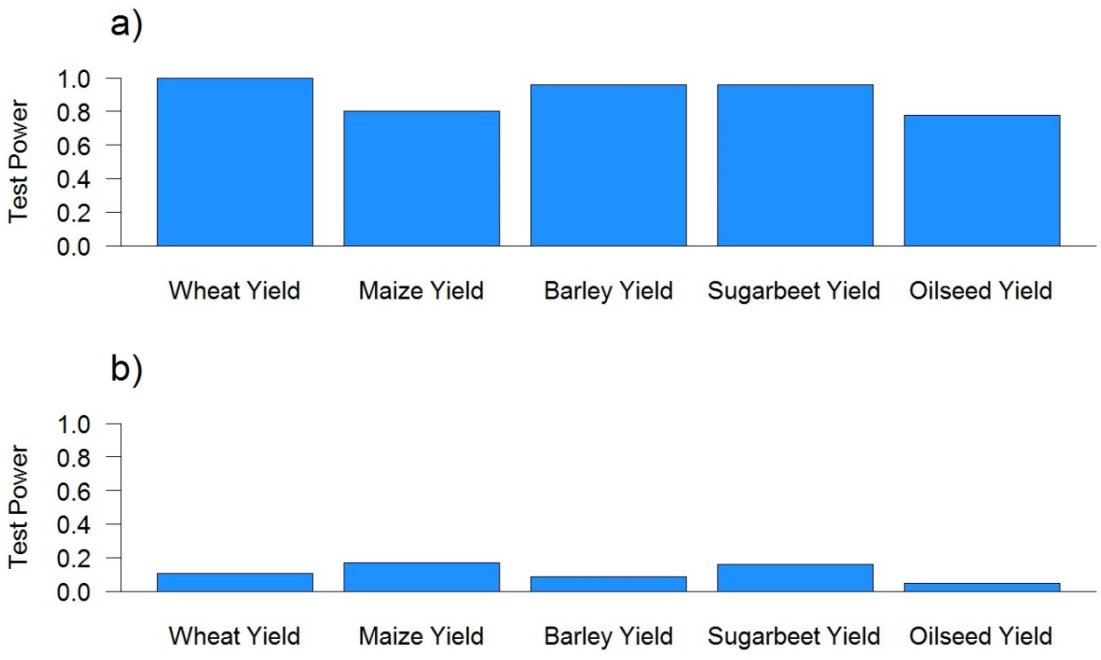

Figure S7: Estimated power of statistical tests for a) the detection of climate change impacts (Test 1) and b) the detection of adaptation to those impacts (Test 2) for observed values of climate trends, response functions, and baseline climate for 5 crops in Europe (Table S4). Power is estimated using 500 simulations for each crop and, for each simulation, inference is made using 500 bootstraps. Each simulation uses 125 independent data points, which may overestimate the number of independent data points in our dataset because of spatial autocorrelation. These should therefore be considered upper bounds for the true power of these tests for this dataset.

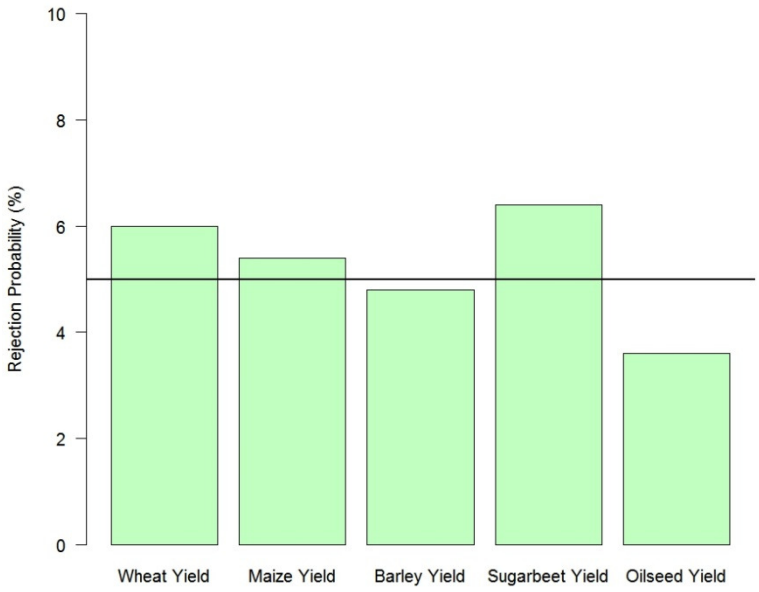

Figure S8: Probability of rejecting a true null hypothesis for Test 2 (the detection of climate change adaptation) estimated using 500 simulations for all crop yield response curves. The horizontal black line shows the desired test size of 5%. Rejection probabilities are close to 5% for all crops, though the test may be slightly conservative for oilseed yields.

Supplementary Results

Panel A	Wheat Yield		
	(1)	(2)	(3)
Regression Coefficient (Beta1)	0.41	0.07	0.22
Standard Error	0.10	0.12	0.29
Test Statistic (Tau1)	4.03	0.57	0.77
P(Tau1|H0)	<0.002	0.06	0.14
Degrees of Freedom	349	339	348
Adjusted R2	0.07	0.20	0.08

Panel B	Maize Yield		
	(1)	(2)	(3)
Regression Coefficient (Beta1)	1.39	0.30	--
Standard Error	0.88	0.24	--
Test Statistic (Tau1)	1.58	1.23	--
P(Tau1|H0)	0.002	0.02	--
Degrees of Freedom	267	260	--
Adjusted R2	0.1	0.22	--

Panel C	Barley Yield		
	(1)	(2)	(3)
Regression Coefficient (Beta1)	0.50	0.39	0.50
Standard Error	0.34	0.43	0.32
Test Statistic (Tau1)	1.47	0.91	1.24
P(Tau1|H0)	0.012	0.02	0.01
Degrees of Freedom	341	331	340
Adjusted R2	0.06	0.11	0.04

Panel D	Sugarbeet Yield		
	(1)	(2)	(3)
Regression Coefficient (Beta1)	0.82	0.31	1.31
Standard Error	0.81	0.48	0.38
Test Statistic (Tau1)	1.00	0.65	2.31
P(Tau1|H0)	0.02	0.06	0.01
Degrees of Freedom	183	176	182
Adjusted R2	0.28	0.43	0.30

Table S5: Results of Test 1 for the preferred model (1) and alternative specifications. (2) includes country fixed-effects in Equation 4 (Methods) and (3) shows the effect only of temperature changes, with precipitation changes included as a control (Methods). Because of the limited sensitivity of maize yields to temperature in this region (Figure S3), power for maize yields is much lower than 80% and so specification (3) was not conducted.

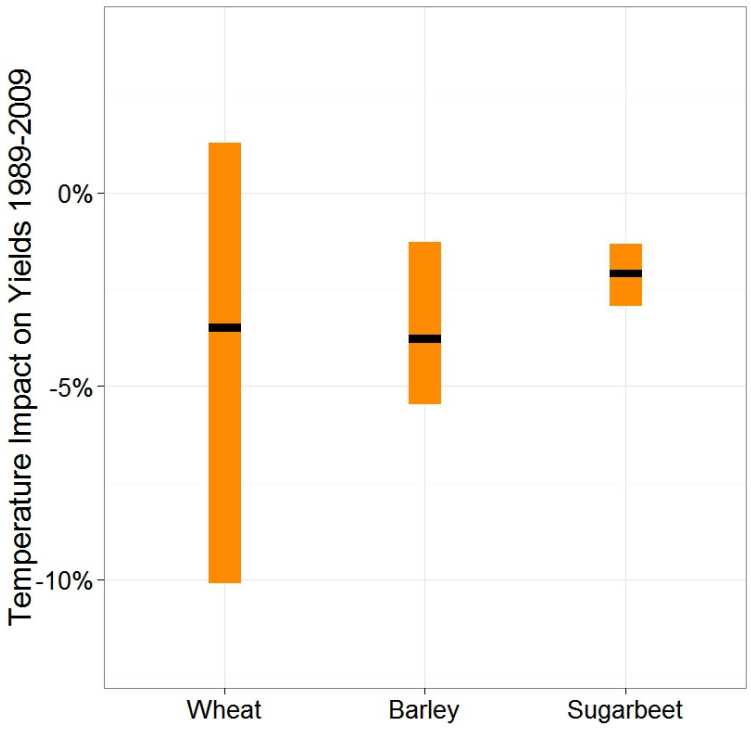

Figure S9: Mean impact of growing-season temperature trends 1989-2009 on wheat, barley, and sugarbeet yields based on the predicted yield trends due to temperature changes and the estimated coefficient shown in Table S5, column 3. The black line shows the point estimate and the orange bar shows the 90% confidence interval obtained by inverting a two-tailed hypothesis test of size 10% (Methods). Impacts are weighted by regional production of the relevant crop 1989-1994 (Methods).

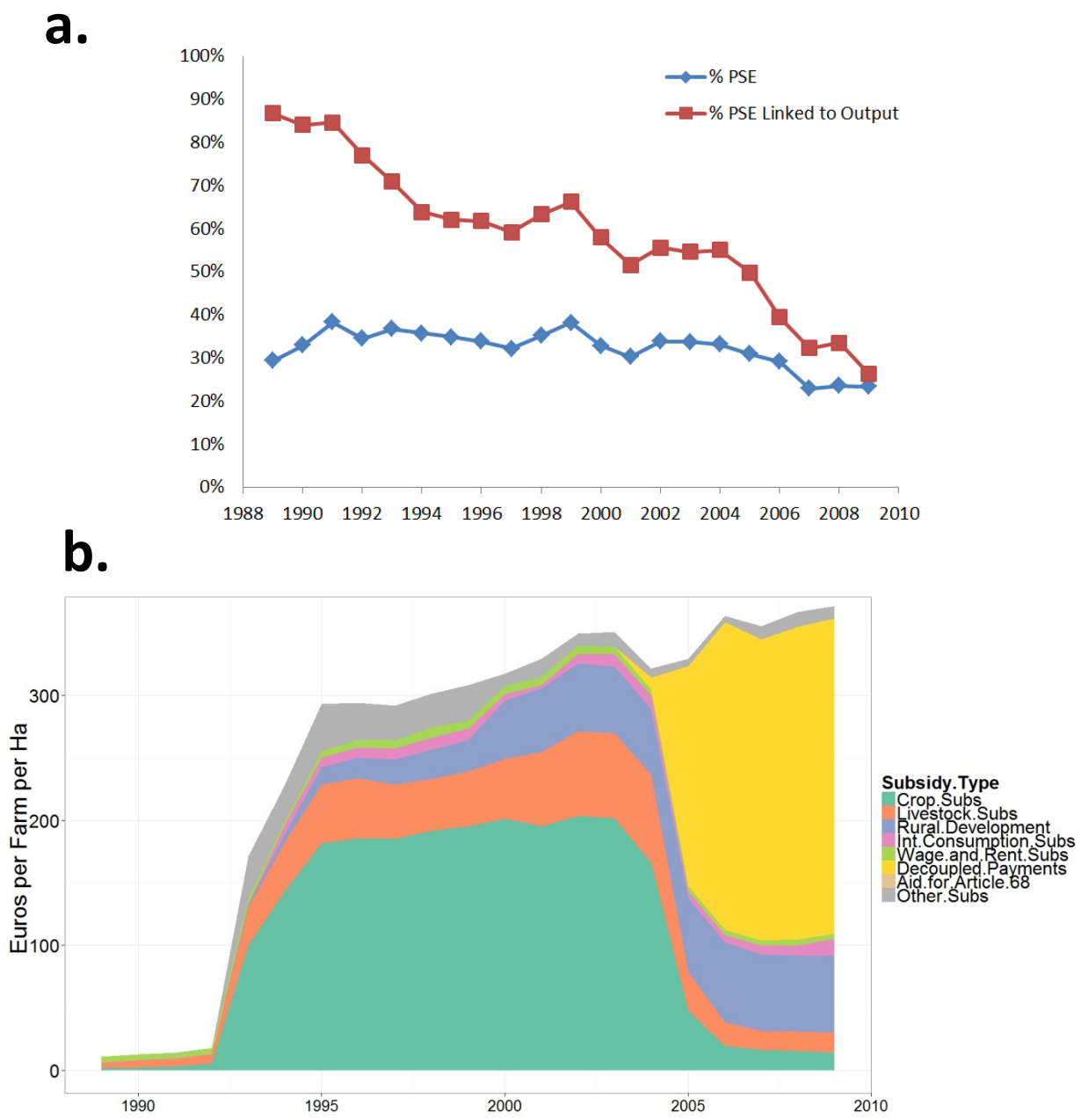

Figure S10: Changes in the form of European farm support. a) Producer Support Equivalent (PSE) in the EU-15, a measure of total taxpayer support to farmers through both price support and subsidy payments. The graph shows both total support as a percentage of farm revenues (%PSE) and the percent of total support linked to commodity production (% PSE Linked to Output) as either price support or payments coupled to production (10). b) Changes in the form of EU subsidy payments. Prior to 1993, agricultural support took the form of direct price supports, not shown in this graph. Between 1993 and 2005, farmers received payments coupled to crop and livestock production (Crop Subsidies and Livestock Subsidies). After 2005, subsidy payments were not based on production but simply on farm size and type (Decoupled Payments) (3).

References

1. Matsuura K, Willmott CJ (2009) Terrestrial Precipitation: 1900-2008 Gridded Monthly Time Series Version 2.01. Available at: http://climate.geog.udel.edu/~climate/.

2. Matsuura K, Willmott (2009) Terrestrial Temperature: 1900-2008 Gridded Monthly Time Series Version 2.01. Available at: http://climate.geog.udel.edu/~climate/.

3. EU (2013) Farm Accountancy Data Network. Available at: ec.europa.au/agriculture/rica/index.cfm [Accessed July 5, 2013].

4. Sacks WJ, Deryng D, Foley JA, Ramankutty N (2010) Crop Planting Dates: An Analysis of Global Patterns. *Glob Ecol Biogeogr* 19:607–620.

5. Van Liedekerke M, Panagos P (2005) *ESDBv2 Raster Archive - a Set of Rasters from the European Soil Database Version 2* Available at: http://eusoils.jrc.ec.europa.eu/data.html.

6. Moore FC, Lobell DB (2014) The Adaptation Potential of European Agriculture in Response to Climate Change. *Nat Clim Chang* 4:610–614.

7. Mendelsohn R, Nordhaus WD, Shaw D (1994) The Impact of Global Warming on Agriculture: A Ricardian Analysis. *Am Econ Rev* 84:753–771.

8. MacKinnon JG (2009) in *Handbook of Computational Econometrics*, eds Belsley DA, Kontoghiorghes J (Wiley, Chichester), pp 183–213.

9. Cameron AC, Gelbach JB, Miller DL (2008) Bootstrap-Based Improvements for Interence with Clustered Errors. *Rev Econ Stat* 90:414–427.

10. OECD (2013) *Agricultural Policy Monitoring and Evaluation 2013: OECD Countries and Emerging Economies* (Paris).